Published in final edited form as:

*Arterioscler Thromb Vasc Biol*. 2019 December ; 39(12): 2492–2504. doi:10.1161/ATVBAHA.119.312707.

# Extracellular miR-92a mediates endothelial cell-macrophage communication

**Ya-Ju Chang**[1], **Yi-Shuan Li**[1], **Chia-Ching Wu**[2,3], **Kuei-Chun Wang**[1], **Tzu-Chieh Huang**[3], **Zhen Chen**[4], **Shu Chien**[1]

[1]Department of Bioengineering and Institute of Engineering in Medicine, University of California, San Diego, La Jolla, CA 92093, United States

[2]Department of Cell Biology & Anatomy, College of Medicine, National Cheng Kung University, Tainan, Taiwan

[3]Institute of Basic Medical Sciences, College of Medicine, National Cheng Kung University, Tainan, Taiwan

[4]Department of Diabetes Complications and Metabolism, Beckman Research Institute, City of Hope, Duarte, CA 91010, United States

## Abstract

**Objective—**Understanding message delivery among vascular cells is essential for deciphering the intercellular communications in cardiovascular diseases. MicroRNA (miR)-92a is enriched in endothelial cells (ECs) and circulation under atheroprone conditions. Macrophages are the primary immune cells in atherosclerotic lesions that modulate lesion development. Therefore, we hypothesize that, in response to atheroprone stimuli, ECs export miR-92a to macrophages to regulate their functions and enhance atherosclerotic progression.

**Approach and Results—**We investigated the macrophage functions that are regulated by EC miR-92a under atheroprone microenvironments. We first determined the distributions of functional extracellular miR-92a by fractionating the intra- and extra-vesicular compartments from endothelial conditioned media and mice serum. The results indicate that extracellular vesicles are the primary vehicles for EC miR-92a transportation. Overexpression of miR-92a in ECs enhanced the pro-inflammatory responses and low-density-lipoprotein uptake, while impaired the migration, of co-cultured macrophage. Opposite effects were found in macrophages co-cultured with ECs with miR-92a knockdown. Further analyses demonstrated that intra-vesicular miR-92a suppressed the expression of target gene Krüppel-like factor 4 (KLF4) in macrophages, suggesting a mechanism by which intra-vesicular miR-92a regulates recipient cell functions. Indeed, the overexpression of KLF4 rescued the EC miR-92a-induced macrophage atheroprone phenotypes. Furthermore, an inverse correlation of intra-vesicular miR-92a in blood serum and KLF4 expression in lesions was observed in atherosclerotic animals, indicating the potential function of extracellular miR-92a in regulating vascular diseases.

**Corresponding authors contact information** Address: Institute of Engineering in Medicine, University of California, San Diego, La Jolla, CA 92093-0435, shuchien@ucsd.edu, telephone number: 858-349-5296.

Disclosures

None.

**Conclusions—**EC miR-92a can be transported to macrophages through extracellular vesicles to regulate KLF4 levels, thus leading to the atheroprone phenotypes of macrophage and hence atherosclerotic lesion formation.

### Keywords

microRNA; endothelial cells; macrophages; atherosclerosis

### Subject code

Basic Science Research; Endothelium/Vascular Type/Nitric Oxide; Inflammation; Vascular biology; Atherosclerosis

## Introduction

Atherosclerosis is a chronic disease driven by maladaptive processes and non-resolving inflammatory responses[1]. At the early stage of pathological progression in atherosclerosis, circulating monocytes are recruited by injured endothelial layer, subsequently, adhere and transmigrate into the subendothelial space. In response to local cytokines and low-density lipoproteins (LDL), infiltrating monocytes differentiate into macrophages (Mϕs), which constitute the primary immune cells accumulated in atherosclerotic plaques[2,3]. The non-resolving inflammation usually results from the imbalance between pro-inflammatory and pro-resolving responses caused by Mϕ heterogeneity, which has been found to play an important role in atherosclerotic lesion development[4]. Therefore, the interaction between immune cells and dysfunctional endothelial cells (ECs) is recognized as an early event for the initiation of inflammatory cascades and an important contributor to the pathological progression of atherosclerotic vascular diseases.

Activation of inflammatory responses in monocyte-derived Mϕs is critical for the nascent atherosclerotic lesion formation, and this is followed by an extensive spectrum of signal networks and functions through the alterations of pro-inflammatory and pro-resolving responses[5]. There are different functions in pro-inflammatory and pro-resolving Mϕs, including inflammatory responses, pathogen clearance, efferocytosis, LDL uptake, and migration ability[6–8]. Notably, the pro-inflammatory Mϕs are classified into classically active Mϕs with the secretion of pro-inflammatory cytokines or chemokines, such as tumor necrosis factor-α (TNF-α) and interleukin-6 (IL-6)[9]. A high capacity of LDL uptake in pro-inflammatory Mϕs has been found to accelerate the local inflammatory responses. On the contrary, those Mϕs activated by the alternative pathway with cytokines interleukin (IL)-4 and IL-13 are classified as pro-resolving Mϕs which release anti-inflammatory cytokines and prevent the necrotic core formation by facilitating migration ability[10]. Hemoglobin scavenger receptor CD163 and transforming growth factor-beta (TGF-β) have been demonstrated to participate in signal transduction of anti-inflammatory responses and Mϕ alternative activation[11,12]. In advanced lesions, the imbalance of Mϕs with pro-inflammatory and pro-resolving phenotypes contributes to the expansion of necrotic cores and rupture risk of lesion plaques. In contrast to the advanced lesion, regression lesions have more effective

pro-resolving Mϕs to reduce the accumulation of pro-inflammatory Mϕs by cleaning apoptotic Mϕs from atherosclerotic plaques[4,13].

Emerging biological evidence and bioinformatics survey have revealed that microRNAs (miRs) are released into human plasma and serum to serve as the biomarkers for clinical diagnosis, prognosis, and follow-up monitoring the consequence of treatments[14]. The extracellular miRs retain their stability and avoid degradation by being incorporated into membrane-derived vesicles or bound to circulating proteins, to mediate cells communicating with neighboring or remote cells[15,16]. miR-92a, a member of miR17–92 cluster, is important for cell angiogenesis, apoptosis, migration, and inflammation[17–19]. Endothelial miR-92a is responsive to atheroprone microenvironmental cues, and its expressional level is increased by oscillatory low shear stress and oxidized LDL[20]. Krüppel-like factor (KLF4) is one of the downstream targets of miR-92a. The increase of KLF4 by diminishing miR-92a in ECs promotes EC homeostasis[21,22]. *In vivo* study has shown that systemic inhibition of miR-92a with specific oligomers prevents atherosclerosis in *ldlr−/−* mice[23]. The circulating miR-92a in human serum and plasma correlates positively to atherosclerosis, renal failure, hypertension, and inversely to brown fat activity[24–26], suggesting that miR-92a serves as an extracellular messenger for cell-cell communication in the cardiovascular system.

Given the potential of endothelial miR-92a on Mϕ phenotypic switch, we investigated its role in the communication between ECs and Mϕs. Our current study has demonstrated that (A) miR-92a is transported from atherogenic ECs to Mϕs through extracellular vesicles; (B) the pathophysiologic Mϕ phenotypes, such as inflammatory responses, LDL uptake, and impaired migration ability, are induced by intra-vesicular miR-92a; and (C) that Mϕ KLF4 is targeted by endothelial miR-92a. Our studies have demonstrated that endothelial miR-92a modulates Mϕ plasticity under pathophysiologic microenvironments.

## Materials and Methods

The data that support the findings of this study are available from the corresponding and first authors upon reasonable request.

### Antibodies and reagents

Rabbit polyclonal antibody (pAb) against Alix was purchased from System Bioscience. Rat monoclonal antibody (mAb) against CD68 was purchased from Bio-Rad. Anti-alpha smooth muscle actin antibody conjugated with FITC was purchased from Abcam. Rabbit pAb against Flotillin-1 and GKLF (KLF4, H-180), mouse mAb against CD63 (E-12), CD81 (1.3.3.22), β-actin, GAPDH, goat pAb against ICAM-1 (M-19), and goat pAb VCAM-1 (C-19) were purchased from Santa Cruz Biotechnology. Custom miR-92a with Dy547 was purchased from Dharmacon™. Lipofectamine RNAiMAX, Lipofectamine 2000, mirVana miR-92a mimic (Pre-92a), mirVana miR-92a inhibitor (Anti-92a), and control oligonucleotides were purchased from Thermo Fisher Scientific. pcDNA3.1-HA-KLF4 FL was a gift from Michael Ruppert (Addgene plasmid #34593)[27]. miRCURY™ RNA isolation kits for cells and biofluids were purchased from Exiqon. Cel-miR-39, a synthetic *C.elegans* microRNA, served as a spike-in control for all the extracellular miR assays. For more detailed information, please see the Major Resources Table in the Supplemental Material.

### Cell culture

Human umbilical venous endothelial cells (HUVECs) were maintained in medium 199 (M199) with 10% (v/v) fetal bovine serum (FBS, Cell Application, Inc.), 10% endothelial basal medium (EBM, Cell Application, Inc.), 1% (v/v) L-glutamine (Thermo Fisher Scientific) and 1% (v/v/) penicillin-streptomycin (P-S, Thermo Fisher Scientific) supplements. THP-1 cells were maintained in RPMI 1640 media supplemented with 10% FBS, 1% GlutaMax (Thermo Fisher Scientific), and 1% P-S, and differentiated into Mϕs using phorbol-12-mysristate acetate (PMA, 150nM) treatment for 48 hours.

### Peripheral blood mononuclear cell (PBMC) purification and Mϕ differentiation and polarization

Buffy coats from healthy volunteers were purchased from San Diego blood bank, and PBMCs were immediately purified with Histopaque-1077 gradient. Briefly, buffy coat was diluted with PBS and layered on top of Histopaque-1077, followed by 400×g centrifuge for 35 minutes at room temperature. The PBMC-containing interface was gently transferred into a fresh conical tube, rinsed twice with PBS, and pelleted with 250×g centrifugation. PBMCs were maintained in RPMI1640 medium and then differentiated into Mϕs with recombinant human macrophage colony-stimulating factor (M-CSF, 50ng/mL) for 7 days. Mϕs were further polarized by treatments with lipopolysaccharide (LPS, 10pg/mL), interferon gamma (IFNγ, 20ng/mL), interleukin (IL)-4 (20ng/mL), and IL-13 (20ng/mL) for cellular plasticity verifications. For resource information of PBMC, please see the Major Resources Table in the Supplemental Material.

### EC-Mϕ co-culture in static experiments

The EC-Mϕ co-culture was conducted using transwell inserts with 1.0-μm pore size (Corning) in a 6-well plate. HUVECs ($5\times10^4$) were seeded onto the upper compartment of the insert for 24 hours followed by pre-conditioning with shRNA, siRNA, and TNF-α. PBMCs or THP1 cells at the bottom of the 6-well plate were differentiated into Mϕs prior to co-culture assembly (Figure 1A).

### EC-Mϕ co-culture in parallel-plate shear system

Different from static experiments, the ECs for shear studies were cultured at the bottom of the transwell insert, and the THP1- or PBMC-derived Mϕs were cultured on its top (Figure 1D). M199 and RPMI 1640 culture media, with 10% FBS supplement, were used for maintaining ECs and Mϕs, respectively. The inserts were subsequently incorporated into parallel-plate flow chambers and connected to a perfusion system to generate pulsatile shear flow (PS, 12±4 dyn/cm$^2$) and oscillatory shear flow (OS, 0±4 dyn/cm$^2$).

### Isolation of extracellular vesicles (EVs) from media

HUVECs were cultured in culture medium with the 10% exosome-depleted FBS (System Bioscience). The ECs were treated with TNF-α (10 ng/mL, R&D) or subjected to shear flows. The collected media were subjected to 300×g centrifugation for 10 minutes to eliminate cell debris, followed by 100,000×g ultracentrifugation for 90 minutes. The vesicle

(pellet) and vesicle-free (supernatant) fractions were collected. Additional washing steps on the vesicle portion were performed with PBS.

### Transmission electronic microscopy examination of EVs

Immunogold labeling was conducted as previous described[28]. In brief, EVs were fixed with 4% paraformaldehyde and deposited onto electron-microscopy grids. The samples were blocked with 2% BSA for 10 minutes and incubated with anti-CD63, anti-CD81, and anti-LAMP1 for 1 hour. The gold-conjugated-secondary antibodies were subsequently applied for 30 minutes, followed by 1% glutaraldehyde incubation to stabilize the immunoreaction. The grid was dried at room temperature and examined on a JEOL 1200 EXII transmission electron microscope.

### Nanoparticles tracking analysis of EVs

The sizes and numbers of EVs were analyzed by NanoSight LM10-HS (Malvern Instruments). NanoSight LN10-HS characterizes the nanoparticle by referring to the distribution of light scattering intensity.

### Isolation of EVs from animal serum

The sera from ApoE$^{-/-}$ mice fed with normal or Pagien diet for 8 weeks were collected by serum separator tubes with 3,500 rpm centrifugation for 15 minutes. EVs from the collected mice sera were purified with ExoQuick kit (SBI) following the Standard Operating Procedures from the Extracellular RNA Communication Consortium (ERCC) Research Portal.

### Quantitative real-time PCR and miRNA assay

Total RNA was isolated from intra-cellular, intra-vesicular, and extra-vesicular compartments by TRIzol (Thermo Fisher Scientific) or miRCURY™ RNA isolation kits. Quantitative PCR (qPCR) was conducted with iTaq Universal SYBR Green Supermix (Bio-Rad) or Taqman Fast Universal PCR Master Mix (Applied Biosystems) using specific primers and probes. The expressional levels of intracellular miRNA were normalized to the internal control RNU48; and the levels of intra-/extra-vesicular miRNA were normalized to the spike-in control Cel-miR-39.

### Cytokine array

The conditioned media of Mϕs under various experimental conditions were collected and cleaned by 1,500 rpm centrifugation for 10 minutes. The media (1 ml) were mixed with the detection antibodies, and then applied to the cytokine array (R&D) at 4°C overnight. The signals were detected with luminol-based enhanced chemiluminescence (ECL) HRP substrate system (Thermo Fisher Scientific). The grayscale intensity of each dot plot was quantified with Image J, and then normalized to the positive control on each array membrane.

### Migration assay

Transwell migration assay was conducted with 8-μm pore size inserts (Corning). THP1 cells ($1\times10^6$ cells/insert) were seeded onto the top membrane and differentiated into Mϕ for 2 days prior to co-culturing. HUVECs ($0.5\times10^5$ cells/well) were preconditioned with shRNA, siRNA, or TNF-α for 24 hours prior to culturing into 6-well plate. After 24-hour co-culturing, the migratory Mϕs at bottom of the membrane were visualized and quantified by hematoxylin staining.

### Western blot analysis

After experiments, the cells were lysed with RIPA buffer containing 50 mM Tris, pH 7.4, 1% NP-40, 1% deoxycholate, 0.1% SDS, 150 mM NaCl, 5 mM EDTA, 50 mM NaF with protease and phosphatase inhibitors (1 mM PMSF, 1 mM sodium orthovanadate, 10 μg/μL leupeptin, 10 μg/μL aprotinin). The proteins were separated on 10% or 12% SDS-PAGE and then transferred onto nitrocellulose membranes. Non-specific bindings were blocked by 5% BSA in Tris-buffer saline with Tween 20 (TBSt) before incubation with specific primary antibodies against ICAM1, VCAM1, Alix, Flottilin-1, CD81, KLF4, GAPDH, and beta-actin. Appropriate secondary antibodies (Santa Cruz) and ECL HRP substrate system (Thermo Fisher Scientific) were used to detect the signals.

### Atherosclerotic animal model

All animal studies were approved by the Institutional Animal Care and Use Committee (IACUC) of the University of California, San Diego. $ApoE^{-/-}$ mice fed with Paigen diet (15% fat, 1.25% cholesterol, and 0.5% sodium cholate) for 8 weeks were used to examine the levels of miR-92a and Mϕ heterogeneity during atherosclerotic development. The blood was collected via cardiac puncture from the ventricle immediately after the animals having been sacrificed. The vascular tissues were harvested and embedded in Tissue-Tek O.C.T.. For resource and background information of $ApoE^{-/-}$ mice, please see the Major Resources Table in the Supplemental Material.

### Tissue immunohistochemistry assay

Sections (10-μm) of vessel samples were acquired from serial cryosectioning. Tissue sections were blocked with 5 % BSA in PBS, followed by the hybridization of primary antibodies against alpha smooth muscle actin, CD68, and KLF4 at 4°C overnight, followed by Alexa Fluor 647 or 594-conjugated secondary antibodies, and DAPI was used for counterstaining. Fluorescent images were acquired from an epi-fluorescence microscope.

### Statistical analysis

Results were presented as mean±SD from at least three independent experiments. Analyses were performed with Prism GraphPad 8.0.1 (GraphPad Software, USA). *F*-test for equal variance examinations and normality tests were performed before analyzing statistical significance between two groups by unpaired t-test. Two-way ANOVA plus a post hoc Sidak's multiple comparisons test was used to compare among three or more groups. All the data for multi-group statistics passed normality and equal variance test. The univariate

correlation was analyzed by Pearson correlation coefficient. A Two-tailed P value < 0.05 was considered statistical significance.

## Results

### Atherogenic ECs enhanced Mϕs pro-inflammation

To determine the Mϕ responses to cytokine-pretreated ECs, a transwell co-culture system was employed. The human PBMCs were isolated and differentiated into Mϕs by M-CSF for 7 days. The monocytic lineage of the PBMC-derived Mϕs was validated with the positive staining of CD14 (Figure IA). The plasticity of these PBMC-derived Mϕs was assessed by their responses to cytokine treatments. The LPS + IFNγ treatment induced the Mϕ to be round fried-egg-shaped with a low aspect ratio, while IL-4 + IL-13 treatment caused Mϕ to be elongated spindle-shaped with a high aspect ratio, indicating their capacities for polarization[29] (Figure IB). The atherogenic phenotype of ECs was induced by the treatment with TNF-α or OS, as validated by the expressions of ICAM1 and VCAM1 (Figure II).

Atherogenic ECs caused the increases of pro-inflammatory genes including IL-6, IL-1α, IL-1β, TNF-α, and iNOS in co-cultured PBMC-derived Mϕs (Figure 1B). These results suggest that the atherogenic ECs activate Mϕs to trigger inflammatory responses. Such inflammatory responses have also been induced in THP1-derived Mϕs co-cultured with the TNF-α-pretreated ECs (Figure 1C). In addition, we investigated the effects of shear flow-regulated ECs on Mϕs inflammation, by exposing ECs to atherogenic OS or athero-protective PS in a parallel-plate co-culture flow system (Figure 1D). The expression levels of IL-6, IL-1α, IL-1β, TNF-α, CD80, and iNOS significantly increased in both PBMC-derived Mϕs (Figure 1E) and THP1-derived Mϕs (Figure 1F) co-cultured with ECs under OS in comparison to the ones under PS. Collectively, these results indicate that chemical- and mechanical-induced atherogenic ECs exhibit pro-inflammatory effects on Mϕs.

### EC miR-92a is transported to Mϕs via extracellular vesicles

MicroRNA(miR)-92a is reported as an atheroprone miR involved in inflammasome activation in ECs[21]. To explore whether endothelial miR-92a is the mediator for atherogenic EC-induced Mϕs inflammation, we investigated miR-92a biogenesis (pri-miR-92a and mature miR-92a) in co-cultured ECs and Mϕs. The pri-miR-92a in the co-cultured ECs increased markedly under TNF-α treatment or OS exposure, but there was no change of pri-mi-92a in the co-cultured Mϕs (Figures 2A and 2B); whereas the levels of mature miR-92a were significantly increased in both ECs and Mϕs (Figures 2C and 2D). These findings suggest that EC-Mϕ co-culture does not induce biogenesis of miR-92a in Mϕ and that the increase of mature miR-92a in Mϕs is transported from the co-cultured ECs.

To investigate the routes for EC miR-92a transportation to Mϕs, we fractionated EC conditioned media (CM) of ECs subjected to TNF-α or OS using sequential ultracentrifugation to pellet the extracellular vesicles (EVs) and obtain the EV-free supernatant (Figure III). The EVs were confirmed by their physical features with particle diameters ranging from 60 to 240nm (classic sizes of microvesicles and exosomes; Figure IVA) and EV markers (CD63, CD81, and LAMP1) immunogold labeling on intact EVs with

toroidal shape (Figure IVB). Additionally, ELISA reader demonstrated that EV markers, CD63 and CD81, are predominantly presented in EV pellet but not in the supernatant (Figure IVC to IVF). RNAs were isolated from the pellets (intra-vesicular RNA) and the supernatant portion (extra-vesicular RNA). In the time-course assessments, both intra- and extra-vesicular miR-92a levels were elevated in ECs subjected to TNF-α for 48 and 72 hours, with the intra-vesicular miR-92a levels being significantly higher than those of extra-vesicular miR-92a (Figure 2E). Furthermore, we quantified the percentages of miR-92a in relation to total RNA presented in intra-vesicular and extra-vesicular compartments based on the absolute amount of endothelial miR-92a in each distinct compartment, quantified by integrating the miR-92a levels and medium volume as dilution factors (Figure VA). The TNF-α treatment and OS application had little effects on the RNA distributions in the three distinct compartments (Figures VB and VC). However, the results demonstrated that there is a markedly higher percentage of miR-92a in the intra-vesicular than extra-vesicular compartments (Figures 2F and 2G). The unchanged EV secretion numbers (Figures VIA and VIB) and the high percentage of intra-vesicular miR-92a suggest that ECs enrich miR-92a in EVs when exposed to the atheroprone environment.

To determine the functional effects of the transported miR-92a, THP-1-derived Mϕs were treated with the fractionated EVs and supernatant of EC-CM. The EVs enhanced the expressions of pro-inflammatory TNF-α and IL-6, and suppressed that of anti-inflammatory CD163 in Mϕs, in comparison to the treatment with supernatant fraction (Figure VIIA). Further cytokine secretion analyses validated that EVs from cytokine-pretreated ECs enhanced Mϕ pro-inflammatory IL-6, chemokine (C-X-C motif) ligand 1 (CXCL1), complement component 5a (C5a), and IL-1α secretion (Figure VIIB). The induction of miR-92a and pro-inflammatory genes in Mϕs receiving TNF-α treated EC-EVs were decreased by knockdown of miR-92a prior to or during the EV treatments (Figure VIII). Overall, these findings suggested that intra-vesicular miR-92a participates, at least in part, in ECs-to-Mϕs communication and activates the inflammatory responses in Mϕs.

## EC miR-92a enhances atherogenic phenotypes of Mϕ

We examined the role of EC miR-92a in modulating EC-to-Mϕ communication and the consequential alterations of Mϕ phenotypes. The Dy537-labeled EC miR-92a was detected in the Mϕs (Figure 3A). In addition, overexpression of miR-92a in ECs increased the expressional levels of TNF-α and IL-6, and decreased CD163 and TGF-β expressions, in the co-cultured Mϕs (Figure 3B). Complementary experiments showed that knockdown of EC miR-92a reduced the expressional levels of TNF-α and IL-6, and enhanced the CD163 and TGF-β, in the co-cultured Mϕs (Figure 3C).

In addition to the augmented inflammatory responses, alterations of the capacities for migration and LDL uptake are also crucial characteristics for atherogenic Mϕs in regulating atherosclerotic plaque progression. The Pre-92a transfection of ECs led to the decreases of Mϕs migrating through the porous membrane in the transwell co-culture system, and the anti-92a transfection of ECs had opposite effects (Figure 3D). LDL uptake in Mϕs was enhanced by EC miR-92a overexpression and suppressed by EC miR-92a knockdown

(Figure 3E). These findings indicate that EC miR-92a plays a critical role in regulating Mϕ functions.

## EC miR-92a targets KLF4 to modulate Mϕ phenotypes

KLF4 is reported to be a transcription factor in regulating Mϕ plasticity and a target of miR-92a in ECs[22,30]. We investigated if the miR-92a transported from EC to target Mϕ KLF4 and hence to regulate Mϕ phenotype. We first demonstrated that the atherogenic ECs significantly reduced KLF4 in co-cultured Mϕs (Figures 4A and 4B). In addition, the miR-92a-overexpressed ECs significantly reduced the Mϕ KLF4 levels, while the miR-92a knockdown in ECs increased KLF4 expressions (Figures 4C and 4D). These results showed that the EC miR-92a indeed targeted KLF4 expression in Mϕs. To further validate miR-92a transport, Mϕ KLF4 levels were examined under treatments with either the intra-vesicular or the extra-vesicular components isolated from CM of atheroprone ECs. KLF4 was significantly reduced, at both RNA (Figure 4E) and protein (Figure 4F) levels, in the Mϕs treated with intra-vesicular component compared with extra-vesicular component. Moreover, EVs isolated from CM of Pre- or Anti-miR-92a transfected ECs validated the role of intra-vesicular miR-92a in regulating Mϕ KLF4 (Figure 4G and 4H).

To understand the role of KLF4 in mediating the EC miR-92a modulation of Mϕ phenotypes, we manipulated the expressional levels of KLF4 (Figures 5A to 5D) in Mϕs prior to co-culture with miR-92a-overexpressed ECs. The overexpression of Mϕ KLF4 attenuated the EC miR-92a-induced pro-inflammatory genes, while elevated the anti-inflammatory genes IL-10, Arg-1, and Fizz1 (Figure 5E). The knockdown of Mϕ KLF4 enhanced EC miR-92a-induced pro-inflammatory genes, while significantly decreased the EC miR-92a-induced anti-inflammatory genes (Figure 5F) In addition, the EC miR-92a-induced LDL uptake and impairment of Mϕ migration were significantly reversed by KLF4 overexpression and enhanced by KLF4 knockdown (Figure 5G and 5H). These results suggest that KLF4 acts as a functional regulator for EC miR-92a to modulate Mϕ functions and that the inhibition of KLF4 by EC miR-92a leads to Mϕ phenotypic changes toward atherogenic phenotypes.

## Circulating miR-92a level is inversely related to KLF4 expression in Mϕs in atherosclerotic lesions

Circulating miR-92a is identified as a potential biomarker for cardiovascular-related diseases, including chronic kidney disease and hypertension[24,25]. Therefore, we study on the association between circulating miR-92a and Mϕs in atherosclerotic lesions to provide valuable information on the mechanism of circulating biomarkers in lesion formation. We found that the intra-vesicular miR-92a was significantly increased in mice fed with Paigen diet when compared to that from mice fed with normal diet (Figure 6A). Integrity of EVs from mice sera were analyzed by phospholipid, CD63, CD81, and size distributions across fractions using NAP-5 size exclusion chromatography (Figures IXA–D, GE Healthcare Life Sciences). The miR-92a was primarily detected in the fractions with CD63 and CD81 expressions (Figure IXE). The *in vivo* evidence supported our *in vitro* finding that miR-92a is enriched in EVs under atherogenic conditions. The characterization of the atherosclerotic lesion at the aorta inner curvature demonstrated massive Mϕ infiltration and high

heterogeneity of smooth muscle cells (SMCs), as well as the necrotic cores (Figures XA and XB). The KLF4 expression in the lesion Mϕs shows an inverse correlation with circulating miR-92a (Figure 6B). Double staining of the lesions also revealed the reversal expression patterns of miR-92a and KLF4 (Figure XI), suggesting the potential regulatory role of extracellular miR-92a in targeting Mϕ KLF4 in atherogenesis.

## Discussion

Cell-to-cell communications are important processes for both physiological and pathological responses. In the pathogenesis of vascular diseases, the dynamics of multicellular responses play critical roles in lesion progression and regression[31]. Extracellular miRs can mediate cell-to-cell communication via their binding to secretory proteins or transport in membrane-formed vesicles[15,32–34]. In pathological processes in blood vessels, extracellular miR-126, miR-143, and miR-145 have been found to mediate cellular communication between ECs and SMCs to regulate SMC turnover or differentiation; while SMCs also can enhance EC proliferation via miR-27a transportation[15,35,36]. In addition, extracellular miR-146a serves as a migration inhibitor between lesion Mϕs to entrap them in atherosclerotic lesions[37]. However, the communication between ECs and Mϕs in the pathological progression of vascular diseases remains unclear.

Among the small non-coding RNAs, miR-92a exerts its effects on physiological responses in a pleiotropic manner that regulates inflammation, cell cycles, and adhesion in cell and tissue levels[21,38,39]. In this study, we have demonstrated that miR-92a-containing EVs from ECs modulates Mϕ functions and phenotypes through the mechanism of targeting KLF4 (Figure 7). Our results showed that atherogenic ECs with high miR-92a expression (Figures 2C and 2D) caused the up-regulation of inflammatory genes in co-cultured Mϕs (Figure 1), suggesting that the inflammatory responses of Mϕs can be induced by EC miR-92a. Of note, we found the level of intra-vesicular miR-92a was markedly increased (Figure 2) without altering the amount of total RNA in EVs (Figure V) or the numbers of EV secreted from atherogenic ECs (Figure VI). These results suggest the existence of a mechanism to enwrap miRs into EVs in response to atheroprone stimuli. Our current data revealed that extracellular miR-92a is transported from ECs to Mϕs with significantly higher abundance in intra-vesicular compartment compared to the extra-vesicular compartment (Figure 2E). Moreover, the increases of inflammatory genes and cytokines were determined in Mϕs when treated with the intra-vesicular compartment from EC-CM; this further validates that the uptake of EV miR-92a is functional in modulating Mϕ phenotypes.

We investigated the effect of miR-92a knockdown prior to and during the EC-EV treatments (Figure VIII). The transfection prior to EC-EV treatment showed that inhibition of miR-92a in Mϕs with EC-EV$^{TNF\text{-}\alpha}$ treatment (high miR-92a) was markedly stronger than the one with EC-EV$^{veh}$ (low miR-92a) treatment, indicating the Anti-92a transfection blocked the exogenous EV miR-92a (Figure VIIIA). Furthermore, the inhibitory effects of Anti-92a during EV treatment was stronger than prior to EV treatment (Figures VIIIC), also suggesting that transfection of Anti-92a blocked the exogenous miR-92a in EC-EVs. Indeed, the knockdown of miR-92a prior to and during the EC-EV treatments decreased the EC-EV$^{TNF\text{-}\alpha}$-induced pro-inflammatory gene expression (Figures VIIIB and VIIID).

The cellular composition in atherosclerotic lesions is dynamic and heterogenic at different progressive stages[31]. Mϕs are the major inflammatory cells in lesions, which adapt to microenvironmental cues and contribute to every stages during lesion progression[4]. At the initial stage, lesion Mϕs present a lipid-laden, pro-inflammatory, metabolic, proliferative, and effective pro-resolving phenotype, followed by accelerated apoptosis, elevated pro-inflammatory, and ineffective pro-resolving phenotype in the advanced lesions[4,6,13]. Lesion Mϕs with high heterogeneity maintain the dysfunction of nascent lesions via their capabilities to modulate local inflammation and lipid accumulation, the continuous uptake of lipoproteins by Mϕs leads to foam cells transformation to reinforce the lesion progression toward advanced lesions. Here, we identified that the lipoprotein uptake capacity of Mϕs is increased by co-culture with miR-92a-enriched ECs (Figure 3E), suggesting EC dysfunction sends messages to lesion Mϕs and enhance the foam cell transformation. In addition to lipid-loading, Mϕ migration ability is also reduced by miR-92a-enriched ECs (Figure 3D), and this may result in the accumulation of more Mϕs and foam cells near the dysfunctional ECs.

We demonstrated the EC miR-92a in regulating molecular signaling on Mϕ by detecting a decrease of KLF4 expression in Mϕs when co-cultured with miR-92a-enriched ECs and EVs (Figure 4). Enhancement of KLF4 expressional levels in co-cultured Mϕs exerted reversal effects on EC miR-92a-induced phenotypic changes (Figure 5), suggesting that KLF4 is a critical mediator for the miR-92a signaling from ECs to Mϕs to regulate Mϕ phenotypes. With respect to Mϕ polarization, KLF4 has been reported to robustly induce M2ϕ in peritoneal Mϕs, bone marrow-derived Mϕs, and Kupffer cells[30,40]. Hence, based on our *in vitro* findings and the information of literature, we conclude that the EC miR-92a promotes Mϕs toward the atherogenic phenotype via regulating the KLF4 level in Mϕs. This concept is also validated by our *in vivo* findings that the KLF4 level in lesion Mϕs is inversely correlated with the serum miR-92a level in an $ApoE^{-/-}$ atherosclerotic mouse model (Figures 6 and XI). This is the first time that miR-92a has been demonstrated to serve as a mediator to promote lesion growth via inhibiting the KLF4 expression in lesion Mϕs.

It is shown that circulating miR-92a may associate with multiple carriers, including lipoproteins and microvesicles. Niculescu et al. showed that miR-92a associated with high-density lipoprotein as well as intermediate- and low-density lipoproteins in human sera[16]. The miR-92a has also been found in the endothelial microvesicles isolated from plasma of the coronary artery disease patients to regulate the endothelial functions[41]. These studies support our notion that circulating miR-92a can be an effector in the atherogenesis. We acknowledge the possibility of a false positive result due to non-vesicular miR-92 contamination in the vesicle-enriched fractions arising from the ExoQuick kit isolation method used. We cannot rule out the possibility that ExoQuick may create an artificial lipid complex/aggregate that is composed of lipids and parts of all damaged lipid carriers in the sample (including EVs and non-EVs). A firm conclusion that miR-92 is carried in EVs will require more in-depth follow up studies. Together, these data suggest that miR-92 is carried, at least in part, in vesicles isolated with vesicle-enriched fractions.

In conclusion, our study demonstrated that intra-vesicular miR-92a secreted by ECs plays a critical role in modulating Mϕ inflammation, migration, and lipoprotein uptake to contribute to the subsequent lesion progression. These findings provide new insights into a regulatory

mechanism for extracellular miRs as highlighted by the multi-functional intra-vesicular miR-92a as a robust biomarker for the potential therapeutic target in atherosclerosis-related diseases.

## Supplementary Material

Refer to Web version on PubMed Central for supplementary material.

## Acknowledgments

We greatly appreciate Timo Meerloo for the assistance of EV imaging using JEOL 1200 EXII Transmission Electron Microscope at the Electron Microscopy Facility of UC San Diego.

Source of Funding

This study was supported by funding from Ministry of Science and Technology (MOST) of Taiwan Grant 104-2911-I-006-507 to C.W. and Postdoctoral Research Abroad Program 106-2917-I-564-086 to Y.C., American Heart Association Go Red For Women Strategically Focused Network grant 16SFRN28420000 to Y.C., and the National Institutes of Health Grants HL106579, HL108735, HL121365 to S.C., R00HL122368 to Z.C. and HL135416 to K.W.

## Nonstandard Abbreviations and Acronyms

| | |
|---|---|
| **Pre-92a** | miR-92a mimic |
| **Anti-92a** | miR-92a inhibitor |
| **EVs** | extracellular vesicles |
| **CM** | conditioned media |

## References

1. Tabas I, García-Cardeña G, Owens GK. Recent insights into the cellular biology of atherosclerosis. J. Cell Biol 2015;209:13–22. [PubMed: 25869663]
2. Gisterå A, Hansson GK. The immunology of atherosclerosis. Nat Rev Nephrol. 2017;13:368–380. [PubMed: 28392564]
3. Shi C, Pamer EG. Monocyte recruitment during infection and inflammation. Nat Rev Immunol. 2011;11:762–74. [PubMed: 21984070]
4. Tabas I, Bornfeldt KE. Macrophage Phenotype and Function in Different Stages of Atherosclerosis. Circ Res. 2016;118:653–667. [PubMed: 26892964]
5. Murray PJ. Macrophage Polarization. Annu Rev Physiol. 2017;79:541–566. [PubMed: 27813830]
6. Chinetti-Gbaguidi G, Baron M, Bouhlel MA, Vanhoutte J, Copin C, Sebti Y, Derudas B, Mayi T, Bories G, Tailleux A, Haulon S, Zawadzki C, Jude B, Staels B. Human atherosclerotic plaque alternative macrophages display low cholesterol handling but high phagocytosis because of distinct activities of the PPARγ and LXRα pathways. Circ Res. 2011;108:985–995. [PubMed: 21350215]
7. Vogel DY, Heijnen PD, Breur M, de Vries HE, Tool AT, Amor S, Dijkstra CD. Macrophages migrate in an activation-dependent manner to chemokines involved in neuroinflammation. J Neuroinflammation. 2014;11:23. [PubMed: 24485070]
8. Martinez FO, Gordon S. The M1 and M2 paradigm of macrophage activation: time for reassessment. F1000Prime Rep. 2014;6:13. [PubMed: 24669294]
9. Chinetti-Gbaguidi G, Colin S, Staels B. Macrophage subsets in atherosclerosis. Nat Rev Cardiol. 2014;12:10–17. [PubMed: 25367649]
10. Gordon S Alternative activation of macrophages. Nat. Rev. Immunol 2003. doi:10.1038/nri978.

11. Etzerodt A, Moestrup SK. CD163 and Inflammation: Biological, Diagnostic, and Therapeutic Aspects. Antioxid Redox Signal. 2013;18:2352–2363. [PubMed: 22900885]
12. Gong D, Shi W, Yi S, Chen H, Groffen J, Heisterkamp N. TGFβ signaling plays a critical role in promoting alternative macrophage activation. BMC Immunol. 2012;13:31. [PubMed: 22703233]
13. Rayner KJ. Cell Death in the Vessel Wall: The Good, the Bad, the Ugly. Arterioscler Thromb Vasc Biol. 2017;37:e75–e81. [PubMed: 28637702]
14. Fichtlscherer S, Zeiher AM, Dimmeler S. Circulating MicroRNAs: Biomarkers or mediators of cardiovascular diseases? Arterioscler Thromb Vasc Biol. 2011;31:2383–2390. [PubMed: 22011751]
15. Zhou J, Li Y-S, Nguyen P, Wang K-C, Weiss A, Kuo Y-C, Chiu J-J, Shyy JY, Chien S. Regulation of Vascular Smooth Muscle Cell Turnover by Endothelial Cell-Secreted MicroRNA-126: Role of Shear Stress. Circ Res. 2013;113:40–51. [PubMed: 23603512]
16. Niculescu LS, Simionescu N, Sanda GM, Carnuta MG, Stancu CS, Popescu AC, Popescu MR, Vlad A, Dimulescu DR, Simionescu M, Sima A V. MiR-486 and miR-92a identified in circulating HDL discriminate between stable and vulnerable coronary artery disease patients. PLoS One. 2015;10. doi:10.1371/journal.pone.0140958.
17. Bonauer A, Carmona G, Iwasaki M, Mione M, Koyanagi M, Fischer A, Burchfield J, Fox H, Doebele C, Ohtani K, Chavakis E, Potente M, Tjwa M, Urbich C, Zeiher AM, Dimmeler S. MicroRNA-92a Controls Angiogenesis and Functional Recovery of Ischemic Tissues in Mice. Science. 2009;324:1710–1713. [PubMed: 19460962]
18. Zhang L, Zhou M, Wang Y, Huang W, Qin G, Weintraub NL, Tang Y. MiR-92a inhibits vascular smooth muscle cell apoptosis: Role of the MKK4-JNK pathway. Apoptosis. 2014;19:975–983. [PubMed: 24705900]
19. Daniel JM, Penzkofer D, Teske R, Dutzmann J, Koch A, Bielenberg W, Bonauer A, Boon RA, Fischer A, Bauersachs J, Van Rooij E, Dimmeler S, Sedding DG. Inhibition of miR-92a improves re-endothelialization and prevents neointima formation following vascular injury. Cardiovasc Res. 2014;103:564–572. [PubMed: 25020912]
20. De Winther MPJ, Lutgens E. MiR-92a: At the heart of lipid-driven endothelial dysfunction. Circ Res. 2014;114:399–401. [PubMed: 24481837]
21. Chen Z, Wen L, Martin M, Hsu C-Y, Fang L, Lin F-M, Lin T-Y, Geary MJ, Geary G, Zhao Y, Johnson D a., Chen J-W, Lin S-J, Chien S, Huang H-D, Miller YI, Huang P-H, Shyy JY-J. Oxidative Stress Activates Endothelial Innate Immunity via Sterol Regulatory Element Binding Protein 2 (SREBP2) Transactivation of MiRNA-92a. Circulation. 2014;2. doi:10.1161/CIRCULATIONAHA.114.013675.
22. Fang Y, Davies PF. Site-specific microRNA-92a regulation of Kruppel-like factors 4 and 2 in atherosusceptible endothelium. Arterioscler Thromb Vasc Biol. 2012;32:979–987. [PubMed: 22267480]
23. Loyer X, Potteaux S, Vion AC, Guérin CL, Boulkroun S, Rautou PE, Ramkhelawon B, Esposito B, Dalloz M, Paul JL, Julia P, MacCario J, Boulanger CM, Mallat Z, Tedgui A. Inhibition of microRNA-92a prevents endothelial dysfunction and atherosclerosis in mice. Circ Res. 2014;114:434–443. [PubMed: 24255059]
24. Shang F, Wang S-C, Hsu C-Y, Miao Y, Martin M, Yin Y, Wu C-C, Wang Y-T, Wu G, Chien S, Huang H-D, Tarng D-C, Shiu Y-T, Cheung AK, Huang P-H, Chen Z, Shyy JY-J. MicroRNA-92a Mediates Endothelial Dysfunction in CKD. J Am Soc Nephrol. 2017;28:3251–3261. [PubMed: 28696247]
25. Huang Y, Tang S, Ji-yan C, Huang C, Li J, Cai A, Feng Y. Circulating miR-92a expression level in patients with essential hypertension: a potential marker of atherosclerosis. J Hum Hypertens. 2017;31:200–205. [PubMed: 27629245]
26. Chen Y, Buyel JJ, Hanssen MJW, Siegel F, Pan R, Naumann J, Schell M, van der Lans A, Schlein C, Froehlich H, Heeren J, Virtanen KA, van Marken Lichtenbelt W, Pfeifer A. Exosomal microRNA miR-92a concentration in serum reflects human brown fat activity. Nat Commun. 2016;7:11420. [PubMed: 27117818]

27. Lin C-C, Liu L-Z, Addison JB, Wonderlin WF, Ivanov AV., Ruppert JM. A KLF4-miRNA-206 Autoregulatory Feedback Loop Can Promote or Inhibit Protein Translation Depending upon Cell Context. Mol Cell Biol. 2011;31:2513–27. [PubMed: 21518959]
28. Théry C, Amigorena S, Raposo G, Clayton A. Isolation and characterization of exosomes from cell culture supernatants and biological fluids. Curr Protoc Cell Biol. 2006;Chapter 3:Unit 3.22.
29. McWhorter FY, Wang T, Nguyen P, Chung T, Liu WF. Modulation of macrophage phenotype by cell shape. Proc Natl Acad Sci. 2013;110:17253–17258. [PubMed: 24101477]
30. Liao X, Sharma N, Kapadia F. Krüppel-like factor 4 regulates macrophage polarization. J Clin Invest. 2011;121:2736–2749. [PubMed: 21670502]
31. Lhoták Š, Gyulay G, Cutz JC, Al-Hashimi A, Trigatti BL, Richards CD, Igdoura SA, Steinberg GR, Bramson J, Ask K, Austin RC. Characterization of Proliferating Lesion-Resident Cells During All Stages of Atherosclerotic Growth. J Am Heart Assoc. 2016;5. doi:10.1161/JAHA.116.003945.
32. Rajendran L, Honsho M, Zahn TR, Keller P, Geiger KD, Verkade P, Simons K. Alzheimer's disease beta-amyloid peptides are released in association with exosomes. Proc Natl Acad Sci. 2006;103:11172–11177. [PubMed: 16837572]
33. Pefanis E, Wang J, Rothschild G, Lim J, Kazadi D, Sun J, Federation A, Chao J, Elliott O, Liu ZP, Economides AN, Bradner JE, Rabadan R, Basu U. RNA exosome-regulated long non-coding RNA transcription controls super-enhancer activity. Cell. 2015;161:774–789. [PubMed: 25957685]
34. Camussi G, Deregibus M-C, Bruno S, Grange C, Fonsato V, Tetta C. Exosome/microvesicle-mediated epigenetic reprogramming of cells. Am J Cancer Res. 2011;1:98–110. [PubMed: 21969178]
35. Wang L, Bao H, Wang K-X, Zhang P, Yao Q-P, Chen X-H, Huang K, Qi Y-X, Jiang Z-L. Secreted miR-27a Induced by Cyclic Stretch Modulates the Proliferation of Endothelial Cells in Hypertension via GRK6. Sci Rep. 2017;7:41058. [PubMed: 28106155]
36. Hergenreider E, Heydt S, Tréguer K, Boettger T, Horrevoets AJG, Zeiher AM, Scheffer MP, Frangakis AS, Yin X, Mayr M, Braun T, Urbich C, Boon RA, Dimmeler S. Atheroprotective communication between endothelial cells and smooth muscle cells through miRNAs. Nat Cell Biol. 2012;14:249–256. [PubMed: 22327366]
37. Nguyen M-A, Karunakaran D, Geoffrion M, Cheng HS, Tandoc K, Perisic Matic L, Hedin U, Maegdefessel L, Fish JE, Rayner KJ. Extracellular Vesicles Secreted by Atherogenic Macrophages Transfer MicroRNA to Inhibit Cell Migration. Arterioscler Thromb Vasc Biol. 2018;38:49–63. [PubMed: 28882869]
38. Henique C, Bollée G, Loyer X, Grahammer F, Dhaun N, Camus M, Vernerey J, Guyonnet L, Gaillard F, Lazareth H, Meyer C, Bensaada I, Legrès L, Satoh T, Akira S, Bruneval P, Dimmeler S, Tedgui A, Karras A, Thervet E, Nochy D, Huber TB, Mesnard L, Lenoir O, Tharaux PL. Genetic and pharmacological inhibition of microRNA-92a maintains podocyte cell cycle quiescence and limits crescentic glomerulonephritis. Nat Commun. 2017;8. doi:10.1038/s41467-017-01885-7.
39. Ohyagi-Hara C, Sawada K, Kamiura S, Tomita Y, Isobe A, Hashimoto K, Kinose Y, Mabuchi S, Hisamatsu T, Takahashi T, Kumasawa K, Nagata S, Morishige KI, Lengyel E, Kurachi H, Kimura T. MiR-92a inhibits peritoneal dissemination of ovarian cancer cells by inhibiting integrin α5 expression. Am J Pathol. 2013;182:1876–1889. [PubMed: 23499550]
40. Han YH, Kim HJ, Na H, Nam MW, Kim JY, Kim JS, Koo SH, Lee MO. RORα Induces KLF4-Mediated M2 Polarization in the Liver Macrophages that Protect against Nonalcoholic Steatohepatitis. Cell Rep. 2017;20:124–135. [PubMed: 28683306]
41. Liu Y, Li Q, Hosen MR, Zietzer A, Flender A, Levermann P, Schmitz T, Frühwald D, Goody P, Nickenig G, Werner N, Jansen F. Atherosclerotic conditions promote the packaging of functional MicroRNA-92a-3p into endothelial microvesicles. Circ Res. 2019;124:575–587. [PubMed: 30582459]

## Highlights

- Atherosclerosis is a chronic inflammatory disease, with endothelial dysfunction and macrophage infiltration.
- MiR-92a is significantly enriched in endothelial cells and circulation under atherogenic conditions.
- Endothelial miR-92a is transported to macrophages mainly through extracellular vesicles.
- Enriched intra-vesicular miR-92a enhances macrophage inflammatory responses, lipoprotein uptake, and confines macrophage migration.
- Intra-vascular miR-92a is functional in regulating macrophage functions and phenotypes to promote pathogenesis.

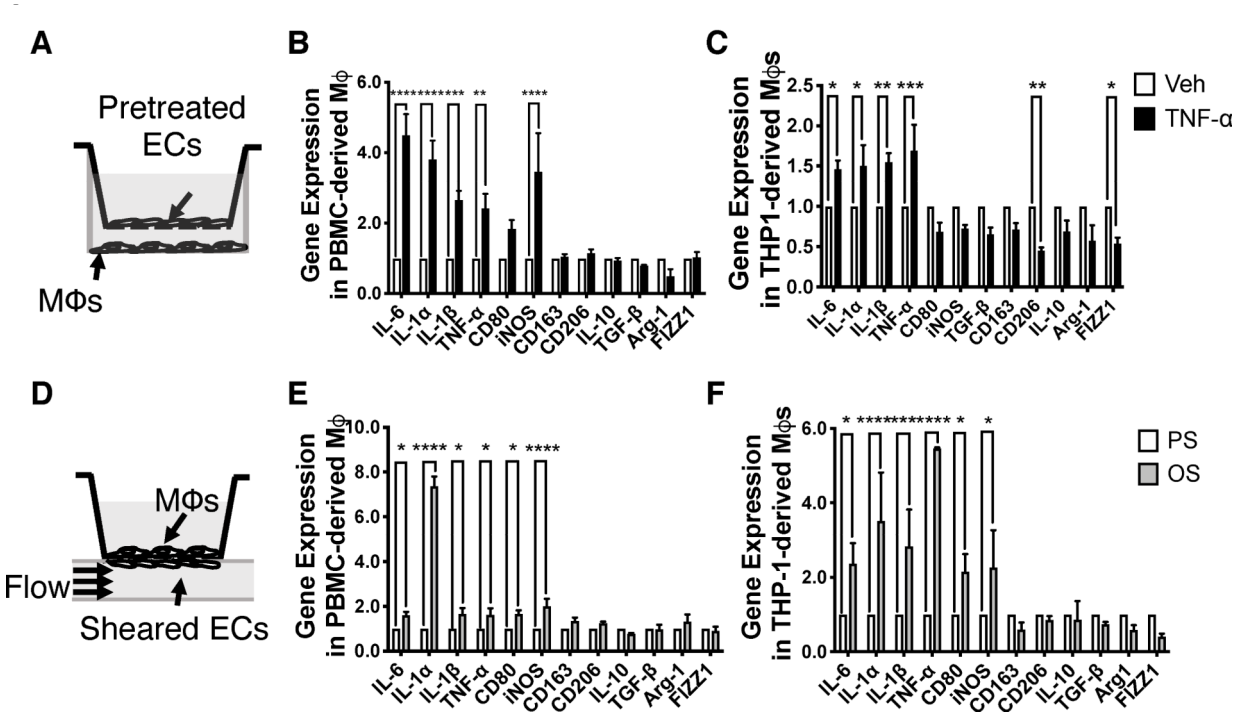


**Figure 1. Macrophages (Mϕs) inflammatory responses are activated by co-culturing with inflamed endothelial cells (ECs).**

(A) In a static co-culture system, Mϕs were co-cultured with TNF-α-pretreated ECs for 24 hours. The relative expression levels of pro-inflammatory (IL-6, IL-1α, IL-1β, TNF-α, CD80, iNOS) and anti-inflammatory (CD163, CD206, IL-10, TGF-β, Arg-1, FIZZ1) genes in (B; n=5) peripheral blood mononuclear cell (PBMC)-derived and (C; n=5) THP-1-derived Mϕs were measured by real-time PCR. (D) In a parallel-plate shear flow system, Mϕs were co-cultured with endothelial monolayer exposed to pulsatile shear (PS, 12±4 dyne/cm$^2$) or oscillatory shear (OS, 0±4 dyne/cm$^2$) for 24 hours. The relative expression levels of pro-inflammatory and anti-inflammatory genes in (E; n=5) PBMC-derived and (F; n=3) THP-1-derived Mϕs were measured by real-time PCR. Statistical analyses were performed with 2-way ANOVA using the program of Prism GraphPad 8.0.1. *$P \leq 0.05$, **$P \leq 0.01$, ***$P \leq 0.001$ ****$P \leq 0.0001$.

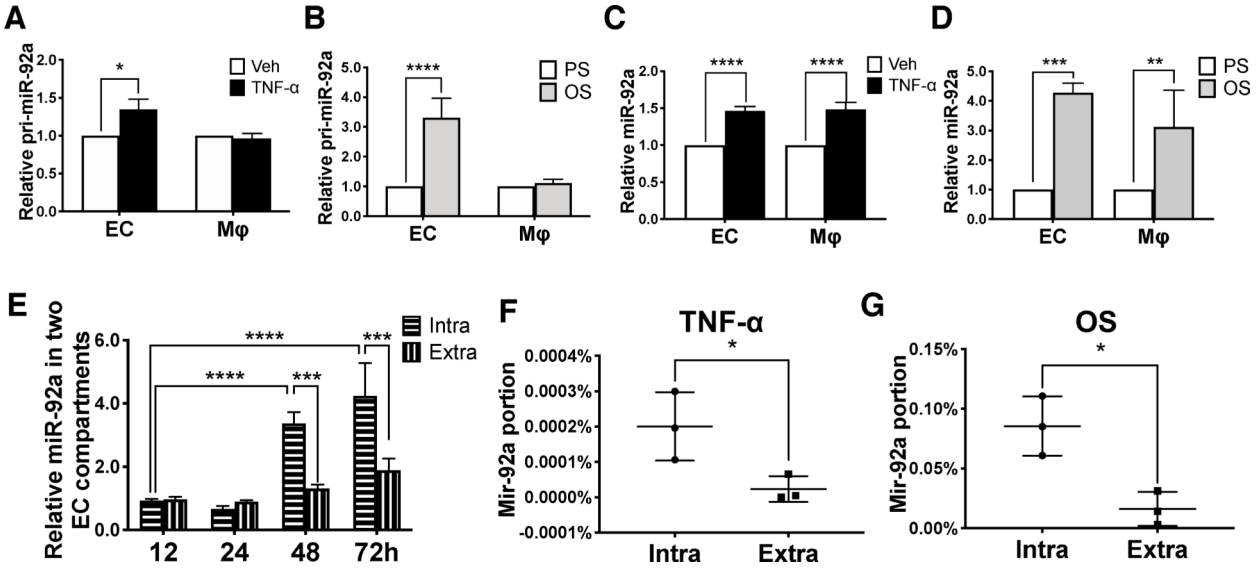


**Figure 2. EC mir-92a is transported via extracellular vesicles (EVs).**

(A&B; n=4&n=3) Levels of Primary miR-92a (Pri-miR-92a) and (C&D; n=3) mature miR-92a in co-cultured ECs and Mϕs were determined by Taqman PCR system. (E; n=3) The levels of intra- and extra-vesicular miR-92a were examined at different time points. (F&G; n=3) Percentages of miR-92a presented in the intra- and extra-vesicular compartments in conditioned media, collected from ECs subjected to TNF-α incubation and OS stimulation, were calculated using a formula described in Figure VC. Statistical analyses were performed by two-way ANOVA or unpaired t-test of Prism GraphPad 8.0.1. $*P \leq 0.05$, $**P \leq 0.01$, $***P \leq 0.001$, $****P \leq 0.0001$.

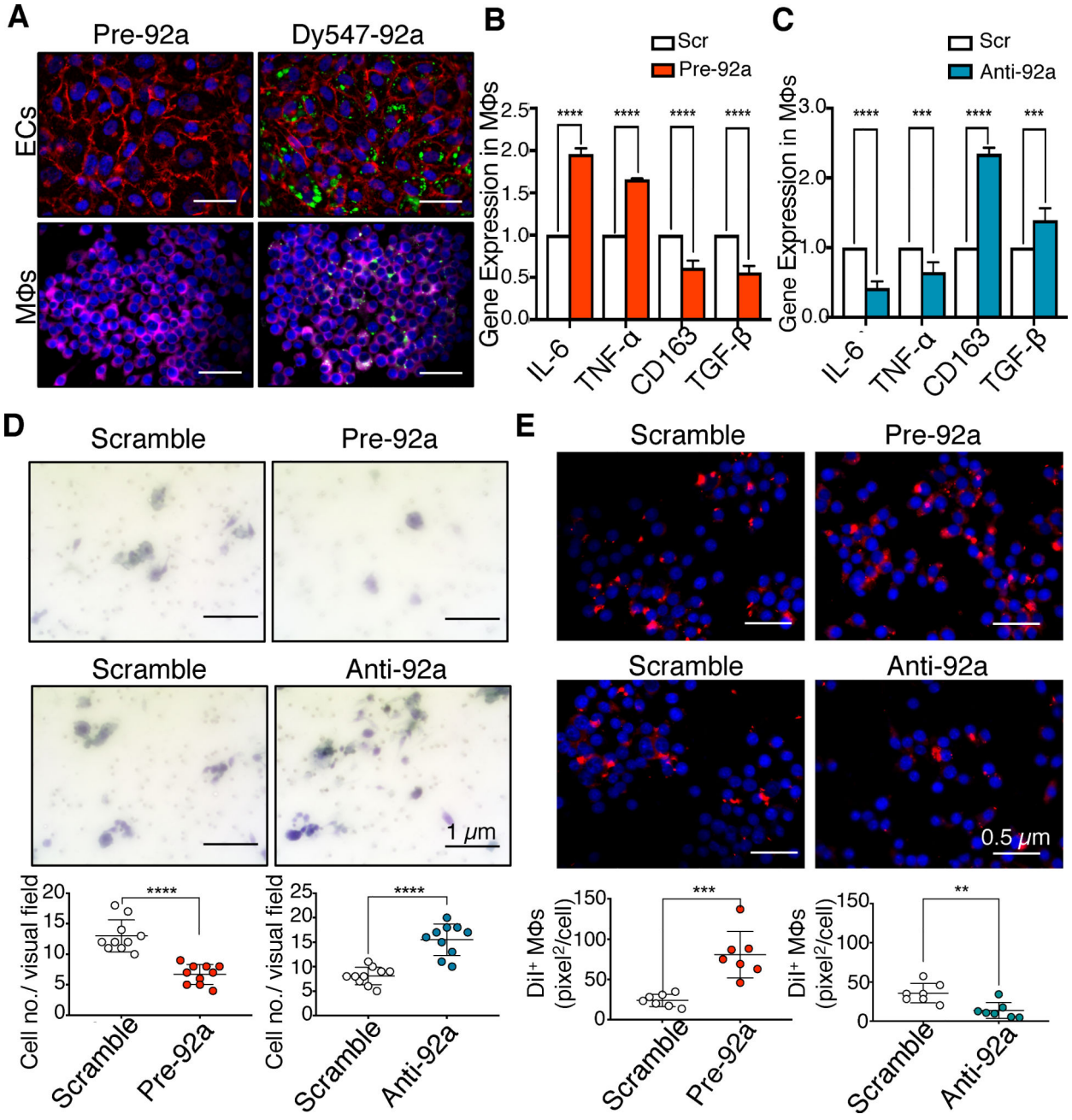


**Figure 3. Modulations of miR-92a in ECs alter Mϕ inflammatory responses and phenotypes.**

(A) The transportation of endothelial Dy547-miR-92a was detected in Mϕs in an EC-Mϕ co-culture system. Co-cultured ECs and Mϕs were stained by VE-cadherin and CD68, respectively. Expressions of pro- and anti-inflammatory genes were measured by real-time PCR in Mϕs co-cultured with ECs with miR-92a (B; n=3) overexpression (Pre-92a) or (C; n=3) knockdown (Anti-92a). (D; n=5) Migrated Mϕs were identified by Hematoxylin staining at the bottom of transwell insert. (E; n=4) Mϕ lipoprotein uptake was quantified by detecting the DiI-labeling low-density lipoprotein (LDL) in Mϕs co-cultured with ECs. Data in B, C, D, and E were mean±SD. Statistical results in B and C were performed by two-way

ANOVA, D and E were calculated by unpaired *t* test. $^{**}P \leq 0.01$, $^{***}P \leq 0.001$, $^{****}P \leq 0.0001$.

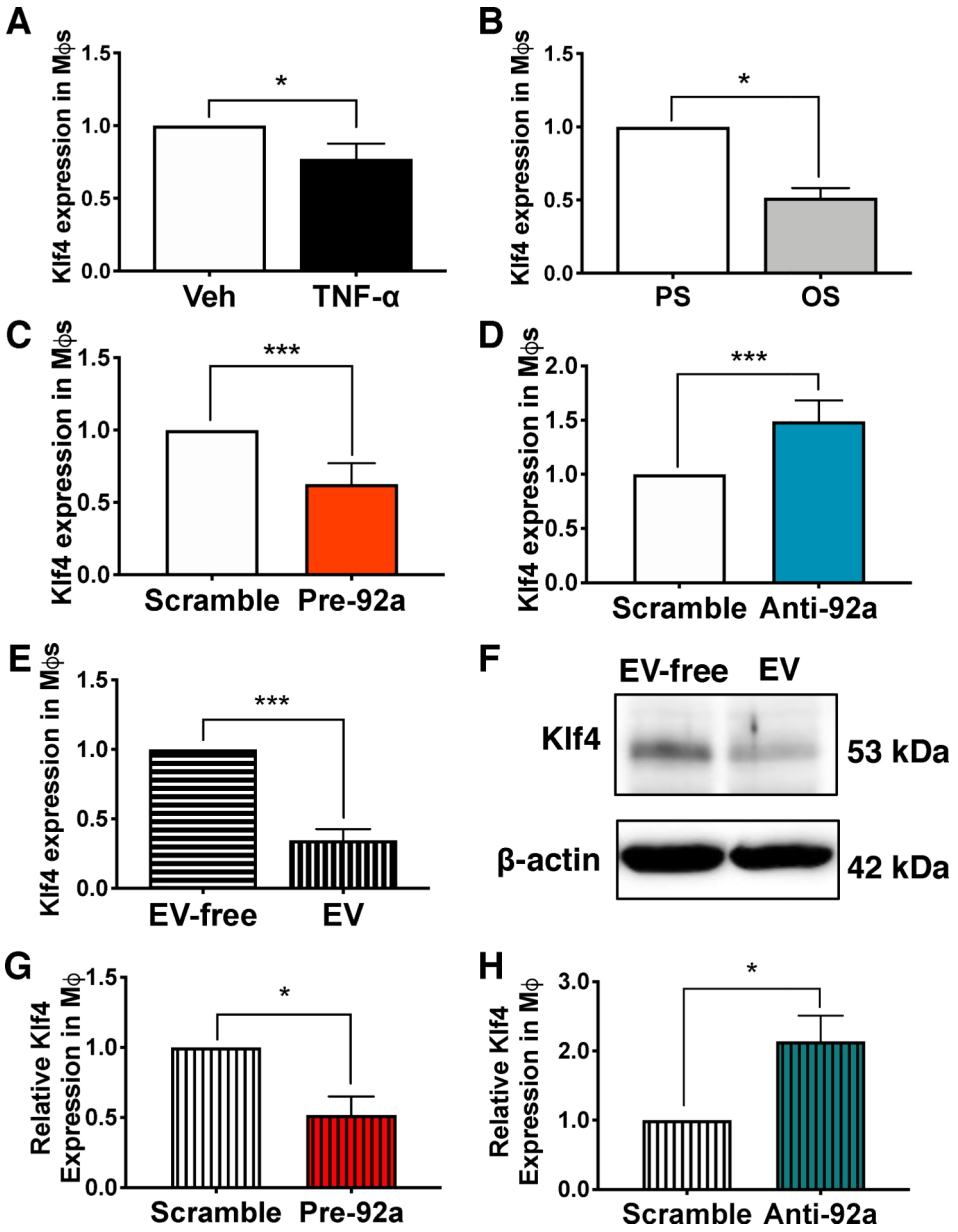


**Figure 4. Krüeppel-like factor (KLF4) is a target of intra-vesicular miR-92a transferred to Mϕs.**

Relative expression levels of KLF4 in Mϕs co-cultured with (A; n=3) TNF-α or (B; n=3) OS stimulated ECs were measured by real-time PCR. KLF4 expressions in Mϕs co-cultured with (C; n=5) Pre-92a or (D; n=5) Anti-92a transfected ECs. KLF4 (E; n=3) RNA and (F) protein levels in Mϕs treated with the EV and EV-free components. KLF4 expressed in Mϕs treated with EVs from (G; n=4) Pre-92a or (H; n=4) Anti-92a transfected ECs. Statistical analyses were performed by unpaired *t* test in A, B, C, D, E, G, and H. $*P \leq 0.05$, $***P \leq 0.001$.

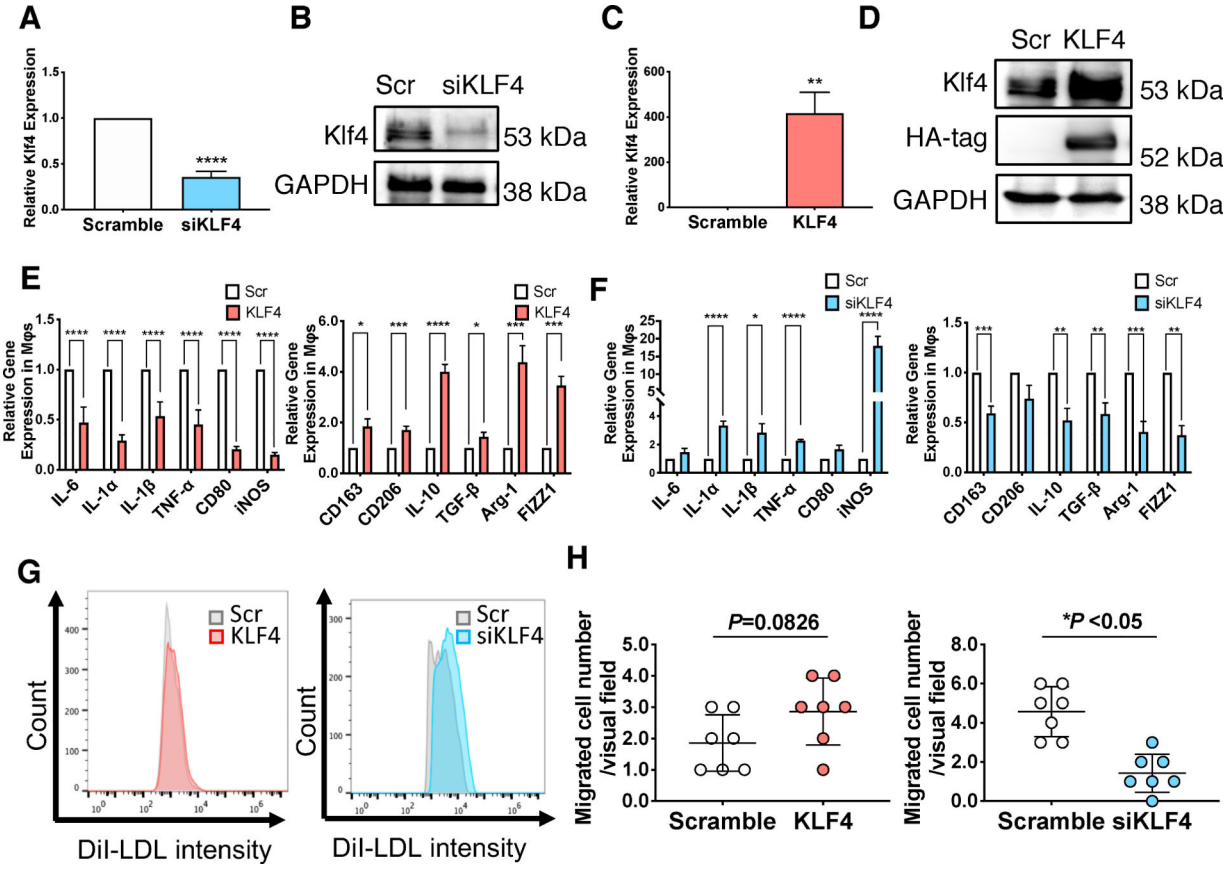


**Figure 5. KLF4 serves as a mediator for EC miR-92a to regulate Mϕ phenotypes.**

Expressional levels of KLF4 RNA and protein were modulated by (A&B; n=3) siRNA and (C&D; n=3) consistently expressing plasmid in Mϕs before co-culturing with ECs. (E&F; n=5) Pro- and anti-inflammatory genes, (G) DiI-LDL uptake, and (H; n=3) migration were evaluated in KL4 overexpressed or knockdown Mϕs co-cultured with miR-92a overexpressed ECs. Statistical analyses were performed by unpaired *t* test in A, C, E, F, and H. *$P \leq 0.05$, **$P \leq 0.01$ ***$P \leq 0.001$, **** $P \leq 0.0001$.

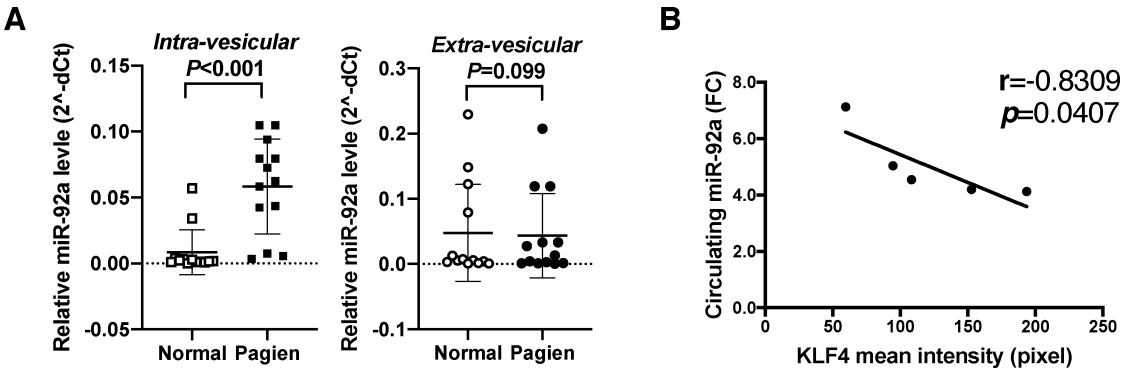


**Figure 6. Intra-vesicular miR-92a in mouse serum is enriched and inversely correlated to KLF4 levels in atherosclerotic lesions.**

(A; n=13) Levels of miR-92a in intra- and extra-vesicular compartments were purified from blood serum of ApoE$^{-/-}$ mice fed with normal or Paigent diet for 8 weeks. Cel-miR-39 was used as a spike-in control. (B; n=5) Tissue segments of aortic arch were harvested from mice after blood isolation, and were fixed and sectioning for KLF4 immunofluorescent staining. Pearson correlation coefficient showed the correlation between intra-vesicular miR-92a and mean intensity of KLF4 in atherosclerotic lesions. Results in A were presented by mean ±SD.

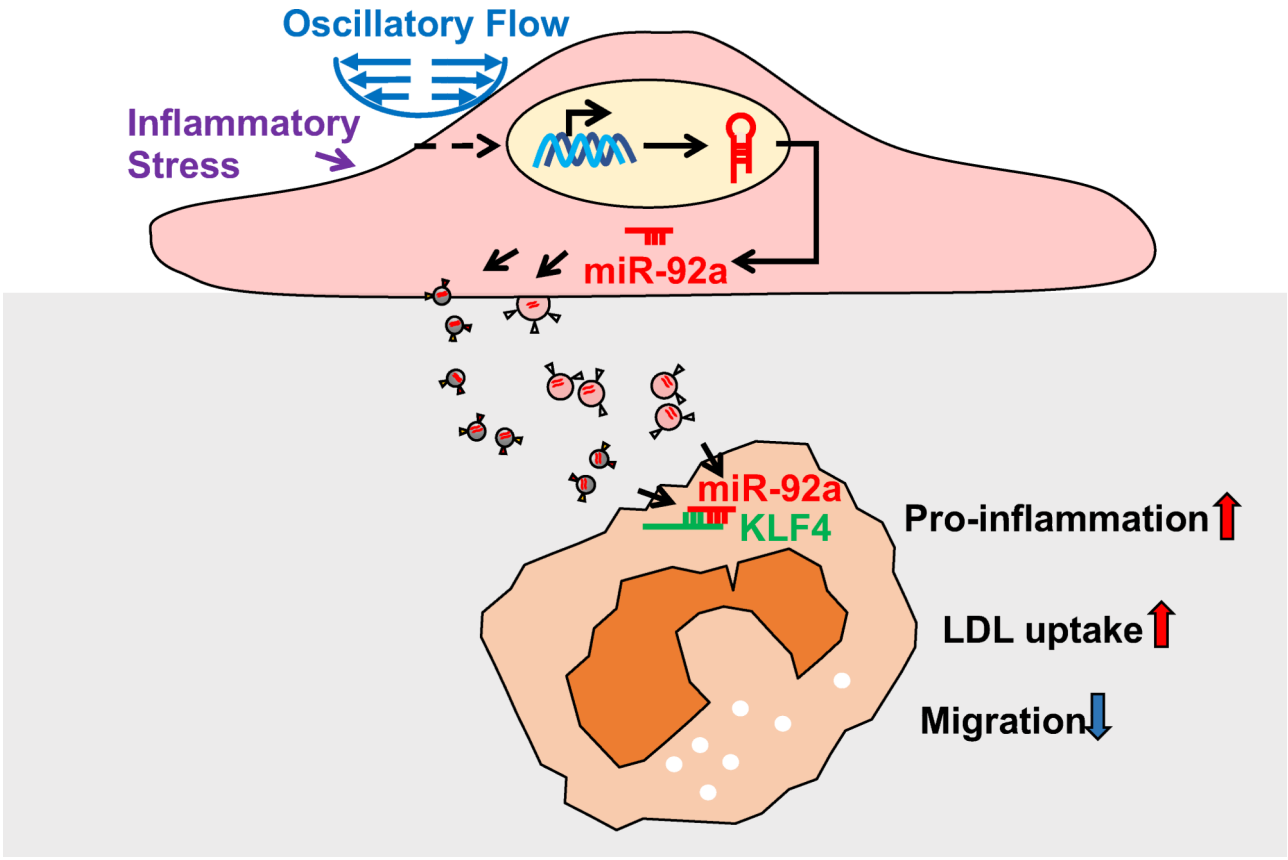


**Figure 7. A working model of EC-to-Mϕ communication during atherogenesis.**

Atheroprone risk factors, OS- and TNF-α, -induced endothelial inflammation result in an extracellular transfer of endothelial miR-92a via EVs to act on Mϕs for the modulation of Mϕ KLF4 expression, which in turn to regulate Mϕ phenotypic changes.